

ORIGINAL ARTICLE

Iran J Allergy Asthma Immunol

April 2025; 24(2):212-236.

DOI: [10.18502/ijaai.v24i2.18149](https://doi.org/10.18502/ijaai.v24i2.18149)

Discovery and Validation of Immune Infiltration-related Genes for the Prognosis of Osteoporosis

Hualiang Xu^{1,2}, Furong Xu³, Lihong Chen¹, Renchun Wu², Hongqing Ge¹, and Aiguo Li¹

¹ Department of Orthopedics, Guangzhou Red Cross Hospital of Jinan University, Guangzhou, Guangdong, China

² Department of Orthopedics, The Third People's Hospital of Bijie City, Bijie, Guizhou, China

³ Department of Nursing, Guangzhou Red Cross Hospital of Jinan University, Guangzhou, Guangdong, China

Received: 26 June 2024; Received in revised form: 1 November 2024; Accepted: 13 November 2024

ABSTRACT

Osteoporosis (OP), a widespread musculoskeletal disorder characterized by fragile bone fractures, has seen increasing attention regarding immune infiltration-related genes. These genes show significant predictive value in solid tumor prognosis and are now being explored for their roles in musculoskeletal diseases. This study identified osteoporosis-associated differentially expressed immune genes (OP-DEGs) by analyzing the overlap between OP-differentially expressed genes and immune genes.

To elucidate the functional implications of these genes, pathway enrichment analysis was conducted using Gene Ontology and KEGG databases. Additionally, Gene Set Enrichment Analysis (GSEA) and Gene Set Variation Analysis (GSVA) were employed to explore underlying mechanisms. A competitive endogenous RNA (ceRNA) network was constructed for critical OP-related immune genes, and immune infiltration analysis investigated micro-environmental characteristics. The diagnostic effectiveness of OP was evaluated using ROC curves. Finally, RT-PCR determined the expression levels of 15 key OP-related immune genes in OP and control groups.

The study identified 29 OP-DEGs. Extensive bioinformatics analysis pinpointed 15 key genes that could serve as potential biomarkers for OP diagnosis. RT-PCR results revealed significantly increased expression of *VEGFA*, *HMOX1*, *RARA*, *CXCL10*, *hsa-miR-129-2-3p*, *OIP5-AS1*, and *HCG18* in the OP group compared to controls.

Our findings suggest that these immune-related genes may predict OP prognosis and offer new perspectives for early prevention and intervention strategies. The identification of specific immune genes involved in OP development highlights their potential as therapeutic targets for further investigation.

Keywords: Bioinformatics; Differentially expressed gene; Immune infiltration; Osteoporosis; Prognosis

Corresponding Authors: Renchun Wu, MD

Department of Orthopedics, The Third People's Hospital of Bijie City, Bijie, Guizhou, China. Tel: (+86 158) 8519 6981, Email: wurenchun@126.com

Hongqing Ge, MD;

Department of Orthopedics, Guangzhou Red Cross Hospital of Jinan University, Guangzhou, Guangdong, China. Tel: (+86 136) 9420 2548, Email: softpiano@163.com

Aiguo Li, MD;

Department of Orthopedics, Guangzhou Red Cross Hospital of Jinan University, Guangzhou, Guangdong, China. Tel: (+86 137) 1140 7200, Email: liaiguo615@163.com

* Hualiang Xu and Furong Xu are co-first authors and contributed equally to this study.

INTRODUCTION

Worldwide, osteoporosis (OP) poses a significant challenge to public health, particularly affecting the older population. According to the International Osteoporosis Foundation (IOF), around 200 million people worldwide suffer from osteoporosis. Every three seconds, an OP-related fracture occurs in more than 9 million people.¹ The incidence of OP in China is 29% for women and 13.5% for men aged 50 and older.² Decreased bone mineral density and quality, along with the degradation of bone tissue's microarchitecture, may result in heightened skeletal fragility and an elevated risk of fractures.³ OP is marked by its widespread occurrence, severe illness rates, increased death rates, and limited public awareness.⁴ This disease has not received sufficient research attention due to its insidious onset and lack of obvious symptoms at an early stage. Specifically, it is difficult to diagnose OP prior to the occurrence of bone fractures. Currently, inhibition of the RANKL-RANK system⁵ and Wnt/ β -catenin signaling⁶ is a major target for the treatment of OP, with denosumab and romosozumab as the respective representative drugs.⁷ However, all available drugs for OP have serious side effects,⁸ and the mechanisms underlying their anti-osteoporotic action are not fully understood.⁹ Hence, innovative therapeutic strategies and efficient preventive measures for OP are critically needed. Achieving this goal requires a deeper understanding of OP's pathogenesis and its possible molecular biomarkers.

Osteoporosis (OP) results from an imbalance in the interactions between bone resorption and formation as part of the bone remodeling cycle. The functions of osteoblasts and osteoclasts, which play a role in maintaining bone balance, are controlled by a wide variety of molecules.¹⁰ Currently, clinical guidelines endorse the use of a spectrum of serum biomarkers that indicate bone turnover and metabolic activity. Included in this group are the following: the type I collagen C-terminal telopeptide; the procollagen I N-terminal propeptide, the amino acids pyridinoline and deoxypyridinoline responsible for cross-linking, parathyroid hormone, osteocalcin, bone-specific alkaline phosphatase, and the tartrate-resistant acid phosphatase variant known as 5b.^{11,12} Nevertheless, these standard protein markers lack tissue specificity for bone and fail to indicate osteocyte function or periosteal metabolic processes.¹³ Furthermore, bone metabolism is

strongly influenced by the immune system.¹⁴ Moreover, the interaction of bone and immune cells could influence the progression of OP.¹⁵ For instance, immune system gene expression profiles, including those of B lymphocytes and monocytes, contribute to the pathogenesis of OP, and crucial genes such as interleukin and its receptors, differentiation cluster molecules, and transforming growth factors can serve as biomarkers for OP.¹⁶⁻¹⁸ Recently, significant research has focused on differentially expressed genes (DEGs) in OP. For example, microRNAs such as *miR-181c-5p*, *miR-497-5p*,¹⁹ *miR-424-5p*,²⁰ and *miR-135b-5p*²¹ are essential molecular regulators in bone metabolism. These microRNAs influence gene expression and are instrumental in bone cell formation. In other words, many microRNAs have been identified as potential biomarkers for osteoporosis. Nevertheless, the intricate characteristics of osteoporosis impede advancements in understanding its etiology, with the underlying molecular processes remaining largely unexplored.

Numerous investigations have been carried out to enhance our comprehension of the molecular pathways of OP by pinpointing various vulnerability genes through a meta-analysis of genome-wide association studies. Nonetheless, the fundamental causal variants and biological regulatory pathways remain largely unexplored.^{22,23} Microarray data analysis can not only identify the key dysfunctional pathways in OP²⁴ but also detect the expression levels of OP-related genes, including mRNAs and lncRNAs.^{25,26} However, the above studies are based on limited data sets, and a small increase in the false positive rate significantly amplifies the analysis results. Consequently, additional in-depth analyses are necessary to pinpoint more dependable biomarkers and rectify these discrepancies.

For this research, we conducted an analysis of gene expression data associated with osteoporosis, drawing from multiple datasets within the GEO (Gene Expression Omnibus) database, and simultaneously extracted genes pertinent to the immune system from the ImmPort repository. Afterward, we carried out an in-depth examination of crucial immune genes related to osteoporosis, which included analyzing gene expression differences, categorizing functions with GO (Gene Ontology), conducting enrichment analysis using GSEA (Gene Set Enrichment Analysis), assessing variability with GSVA (Gene Set Variation Analysis), categorizing immune cell types, constructing ceRNA interaction networks, evaluating diagnostic accuracy,

studying prognostic impact, and analyzing quantitative data. The results indicated that the key immune genes related to OP are closely related to immune cells. These genes can be used as biomarkers of OP and exhibit prognostic value that may lead to new targets for the diagnosis and treatment of OP.

MATERIALS AND METHODS

Data

Gene expression datasets, including GSE56815,²⁴ GSE7158, GSE56116, and GSE100609 were obtained from the GEO database²⁷ using the R software package GEOquery.²⁸ The datasets were then divided into OP and control groups for analysis. Among them, GSE56815 contained 20 premenopausal osteoporotic tissues, 20 premenopausal normal tissues, 20 postmenopausal osteoporotic tissues, and 20 postmenopausal normal tissues; GSE7158 contained 12 osteoporotic tissues and 14 normal tissues; GSE56116 contained ten osteoporotic tissues and three normal tissues; and the validation set GSE100609 contained four osteoporotic tissues and four normal tissues (Supplementary Table S1). Additionally, we retrieved 2,483 genes associated with the immune system from the ImmPort database.²⁹

Osteoporosis-related Differentially Expressed Genes

To analyze the influence of gene expression values on osteoporotic tissues relative to normal tissues, we divided the two data sets into osteoporotic tissues and normal tissues according to the grouping information in the data. We identified DEGs associated with OP using the R package limma.³⁰ The thresholds for statistical significance were set at $|\log FC| > 1.2$ and $p < 0.05$. Taking the intersection of OP-related DEGs and immunological genes yielded OP-related immunological DEGs (OP-DEGs).

Functional Annotations of OP-DEGs

Annotation analysis based on Gene Ontology is frequently utilized in extensive studies of gene function enrichment, encompassing categories such as biological processes (BP), molecular functions (MF), and cellular components (CC).³¹ The KEGG database, a repository extensively employed in the scientific community, archives comprehensive data encompassing genomes, pathways of life processes, medical conditions, pharmaceuticals, and more.³² In our study, the DAVID

Bioinformatics Resources were utilized to aid in the assignment of GO terms and the analysis of KEGG pathways for genes associated with osteoporosis. It is essential to conduct gene-focused ontology enrichment analysis to gain insights into the development of intricate diseases, to detect and prevent major illnesses at an early stage, to explore new avenues for drug discovery, and to evaluate the safety of pharmacological agents. In our research, we applied the R package DOSE³³ for enrichment analysis of OP-DEGs, with statistical significance set at a P value below 0.05.

Gene Set Enrichment Analysis

GSEA assesses gene set enrichment ranked by phenotypic association, to disclose the genetic influence on phenotypes.³⁴ For this research, we retrieved the "C2.kegg.v7.4.symbols" and "c5.go.v7.4.symbols" gene sets from MSigDB and conducted GSEA on the four datasets using the "clusterprofiler" R package.³⁵ A p value < 0.05 was considered statistically significant.³⁶

Gene Set Variation Analysis

The GSVA method, a non-parametric and unsupervised approach,³⁷ facilitates the assessment of gene set enrichment for transcriptome datasets, translating individual gene expression profiles across samples into a gene set-centric format to determine the presence of enriched metabolic pathways. In this study, we obtained the "h.all.v7.4.symbols" gene set from the MSigDB database and performed GSVA on the four datasets to identify differences in functional enrichment between samples.

Immune Infiltration Analysis of OP-DEGs

The immune microenvironment (or tumor microenvironment) is a complex system primarily composed of normal tissue cells, lesional histiocytes, surrounding immune and inflammatory cells, fibroblasts, interstitial tissue, and various cytokines and chemokines. The infiltration analysis of immune cells in cancer tissues plays an important instructive role in disease research, including treatment, prognosis, and prediction.

Employing linear support vector regression, the CIBERSORT algorithm performs the deconvolution of gene expression data for distinct immune cell subtypes. RNA-Seq data are used to estimate the immune cell infiltration in osteoporotic tissues and normal tissues.³⁸ This research employed CIBERSORT to assess immune

cell distribution disparities in osteoporotic versus healthy tissues, correlating OP-DEGs to immune cell presence using Pearson coefficients. The key immune genes associated with OP were identified based on the following criteria: $p < 0.05$ and Pearson correlation coefficients exceeding 0.3 among at least four immune cell genes.

Competitive Endogenous RNA Network Construction

The ceRNA element can compete with RNA. Regulatory networks that involve ceRNA make up the ceRNA regulatory network. In this study, we analyzed miRNAs and lncRNAs that interact with key OP-related immune genes in the post-transcriptional stage.^{39,40} We also used the miRNA database⁴¹ to obtain miRNAs and lncRNAs that interact with key OP-related immune genes. Using Cytoscape software, we visualized the miRNA-lncRNA network for key immune genes associated with OP.⁴²

Validation of Key Osteoporosis-related Immune Genes

The validation set GSE100609 contained four osteoporotic and four normal tissues. As a result, the CIBERSORT algorithm was used to analyze immune infiltration in osteoporotic tissues compared to normal tissues, and a relationship between key osteoporosis-related immune genes and immune cells was found.

Prognostic Association of Key Osteoporosis-related Immune Genes

Utilizing the R package Proc,⁴³ we evaluated the discriminative ability of key OP-associated immune genes by creating ROC curves for five separate datasets and calculating the AUC

for each dataset. Immune genes linked to osteoporosis, demonstrating AUC scores above the 0.5 threshold across all five datasets, were deemed to have prognostic significance.

Bone Mineral Density Assessment and Study Population Selection

Bone mineral density (BMD) was meticulously measured at the femoral neck and lumbar spine (L2-L4) utilizing dual-energy X-ray absorptiometry (DEXA). In accordance with the established guidelines from the World Health Organization (WHO), we defined the thresholds for osteoporosis and non-osteoporosis: a T-

score exceeding -1 standard deviation (SD) was deemed non-osteoporotic, whereas a T-score below -2.5 SD indicated osteoporotic status.

Study Participants

Our study enrolled a total of six subjects, who were carefully stratified into an OP group and a normal control group based on their Bone Mineral Density (BMD) measurements. The inclusion and exclusion criteria were rigorously applied to ensure the validity and reliability of our findings, as outlined below:

Inclusion Criteria:

Postmenopausal women

Exclusion Criteria:

Individuals with conditions potentially affecting bone metabolism, encompassing secondary osteoporosis, chronic bone diseases (e.g., rheumatoid arthritis, osteogenesis imperfecta), metabolic disorders (e.g., diabetes, thyroid diseases), chronic illnesses of internal organs (e.g., liver, kidney), and those currently receiving hormone therapy (e.g., hormone replacement therapy, bisphosphonates, corticosteroid treatment).

All BMD assessments were conducted by a single, highly trained senior technician to maintain consistency and accuracy. Additionally, peripheral blood samples (5 mL) were collected from each participant after a minimum 12-hour fasting period to control for potential confounding factors related to recent dietary intake.

Quantitative Real-time Polymerase Chain Reaction (qRT-PCR) Validation

In total, six individuals, including three in the OP group and three in the normal control group, were recruited for qRT-PCR validation. The qRT-PCR analysis was conducted using the ABI 7500 Real-time PCR Detection System. The protocol commenced with an initial heating at 95°C for a duration of 10 minutes, succeeded by a series of 40 cycles, each comprising heating at 95°C for 15 seconds and a subsequent incubation at 60°C for 1 minute. mRNA expression levels were determined relative to 18s, employing the 2-ΔCt technique, while miRNA levels were normalized to human hsa-U6 as an internal control in the analysis.

Statistical Analysis

Data computation and statistical analysis were performed using R software, particularly version 4.0.2,

accessible at <https://www.r-project.org/>. When comparing continuous variables between two groups, we utilized the Student's t-test for data that followed a normal distribution to establish statistical significance. In contrast, the Mann-Whitney U test (also known as the Wilcoxon rank sum test) was employed for variables that did not conform to a normal distribution. To assess the accuracy of the risk score and its prognostic utility, we employed the pROC package in R to generate ROC curves and calculate AUC values. A p value of less than 0.05 was considered statistically significant, and all tests were conducted as two-tailed tests.

RESULTS

Identification of DEGs

First, we corrected the gene expression values of the selected four groups of data according to the workflow shown in Figure 1. Before correction, the gene expression levels exhibited a larger difference (Figure 1A, 1C, 1E, 1F) than the corrected data, whereas the corrected data showed a more uniform distribution (Figure 1B, 1D, 1F, 1H). To analyze the impact of gene expression values on osteoporotic tissue relative to normal tissue, DEGs was performed using the R package limma, and volcano plots were produced for the DEGs (Figure 2 and Supplementary Table S2). From the GSE56815 dataset, 369 DEGs were identified in the premenopausal group, with 279 genes upregulated and 90 downregulated (Figure 2A). The dataset GSE7158 revealed 2,190 differentially expressed genes (DEGs), consisting of 1,820 upregulated genes and 370 downregulated genes (Figure 2B). In the GSE56116 dataset, 1,103 DEGs were identified, with 738 genes showing upregulated and 365 genes showing downregulated (Figure 2C). In the postmenopausal group of GSE56815, 217 DEGs were detected, of which 117 genes exhibited upregulation and 110 genes exhibited downregulation (Figure 2D). By analyzing DEGs across these datasets, we obtained 205 OP-related DEGs. When intersecting these with 2,483 immune genes resulted in 29 OP-DEGs.

GO Functional Annotation and KEGG Pathway Enrichment Analysis

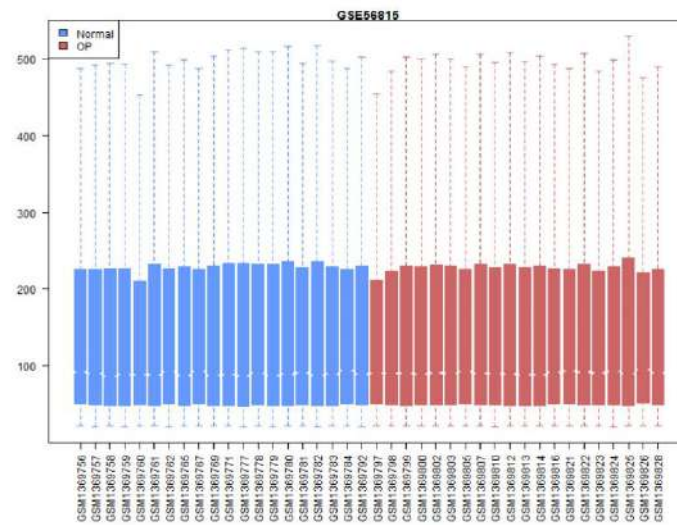
To analyze the relationship between OP-DEGs and biological processes (BP), molecular functions (MF), cellular components (CC), and biological pathways, we first performed GO enrichment analysis of these genes

(Figure 3A and Supplementary Table S3). The analysis revealed that OP-DEGs were primarily involved in several key areas, including immune system reactions, Fc-epsilon receptor pathways, inflammation, ventricular cardiac muscle cell differentiation, RNA polymerase II transcription enhancement, C-type lectin receptor signaling, cell proliferation, cytokine signaling, NF-kappa B activity regulation, and adaptive immune response, all linked to BP, as depicted in Figure 3B. In terms of CC, DEGs showed enrichment in multiple cellular regions, including the plasma membrane, integral components of membranes, regions outside the cell, the outer side of the cell's plasma membrane, extracellular areas, cytoplasm near the cell nucleus, dendrites, complexes of T cell receptors, chromatin within the cell nucleus, and specialized regions of the cell membrane (Figure 3C). Regarding MF, the OP-DEGs exhibited enrichment in enzyme binding, receptor binding, cytokine activity, retinoic acid-responsive element binding, retinoic acid receptor activity, antigen binding, protein binding, protein kinase B binding, heparin binding, and chemokine receptor activity (Figure 3D).

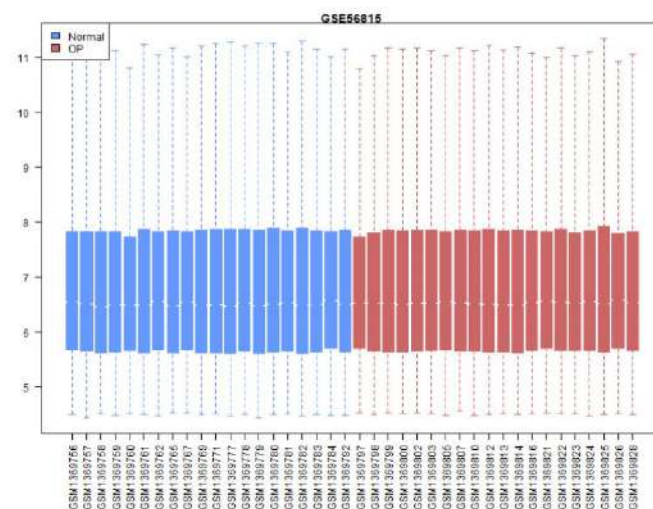
The KEGG enrichment analysis identified significant enrichment of OP-DEGs across various pathways, including Cytokine-cytokine receptor interaction, Chemokine signaling pathway, HTLV-I infection, Pathways in cancer, B cell receptor signaling pathway, Influenza A, Tuberculosis, NF-kappa B signaling pathway, Toll-like receptor signaling pathway, and Toxoplasmosis, among others. Remarkably, the pathway associated with Cytokine-cytokine receptor interaction showed the highest level of significance among all the enriched pathways (Figure 3F). Moreover, we analyzed the diseases related to the OP-DEGs and found that these genes were enriched in Behcet's syndrome, thyroiditis, dengue fever, pulmonary emphysema, malignant neoplasm of the mouth, bronchiolitis, metastatic melanoma, classical Hodgkin's lymphoma, influenza, lung diseases, and other diseases (Figure 3).

Immune Infiltration Genes Linked to Osteoporosis Prognosis

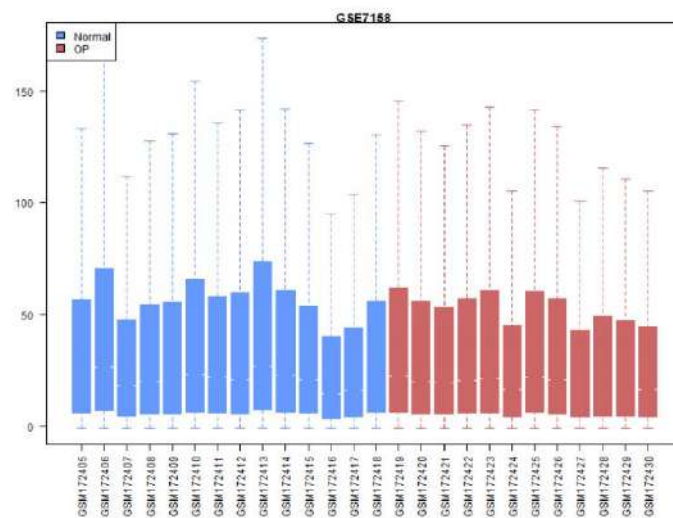
A



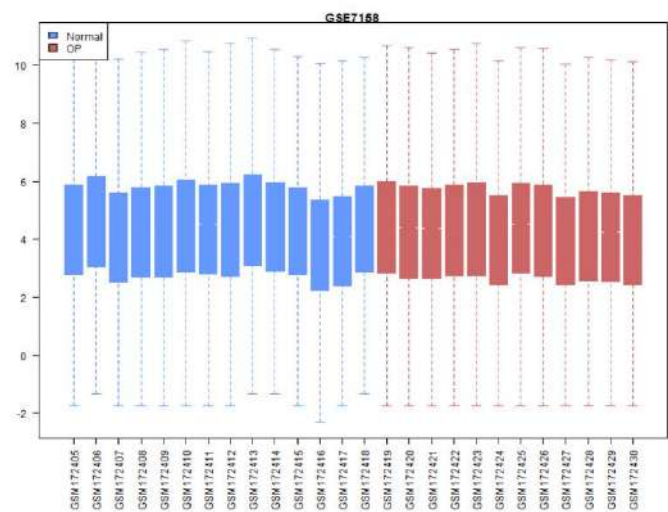
B



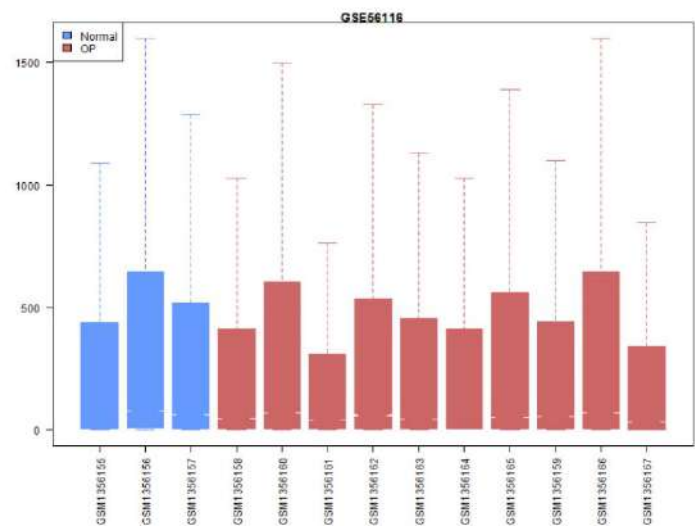
C



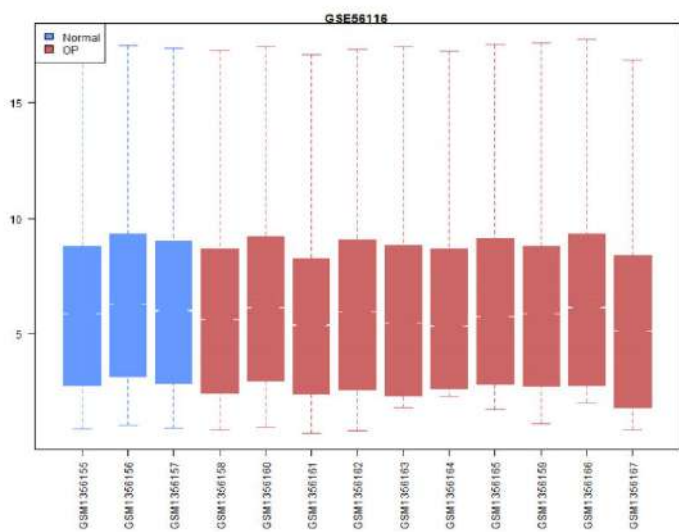
D



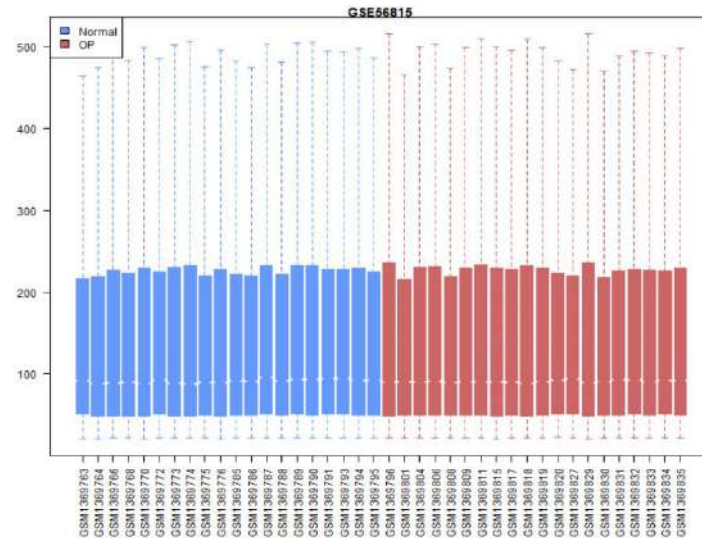
E



F



G



H

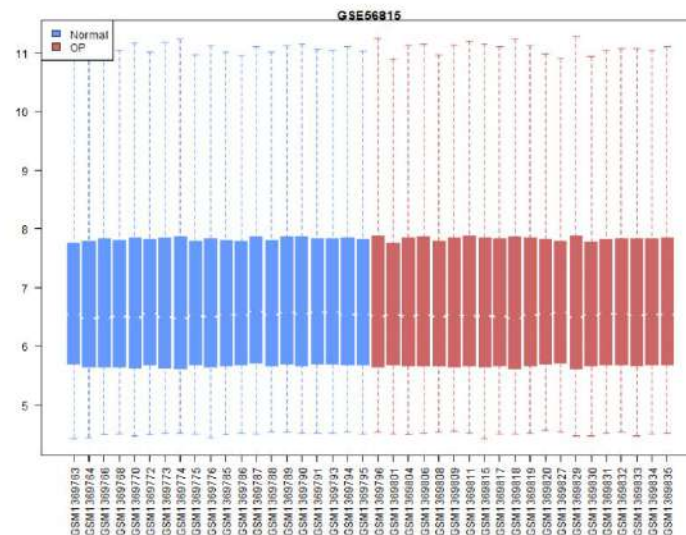


Figure 1. Correction of osteoporosis-related data. Patient ID is shown on the abscissa, and gene expression level is shown on the ordinate. Blue symbols represent osteoporosis tissue, and red symbols indicate normal tissue. Panels A, C, E, and G display pre-correction data, whereas panels B, D, F, and H show the corrected data.

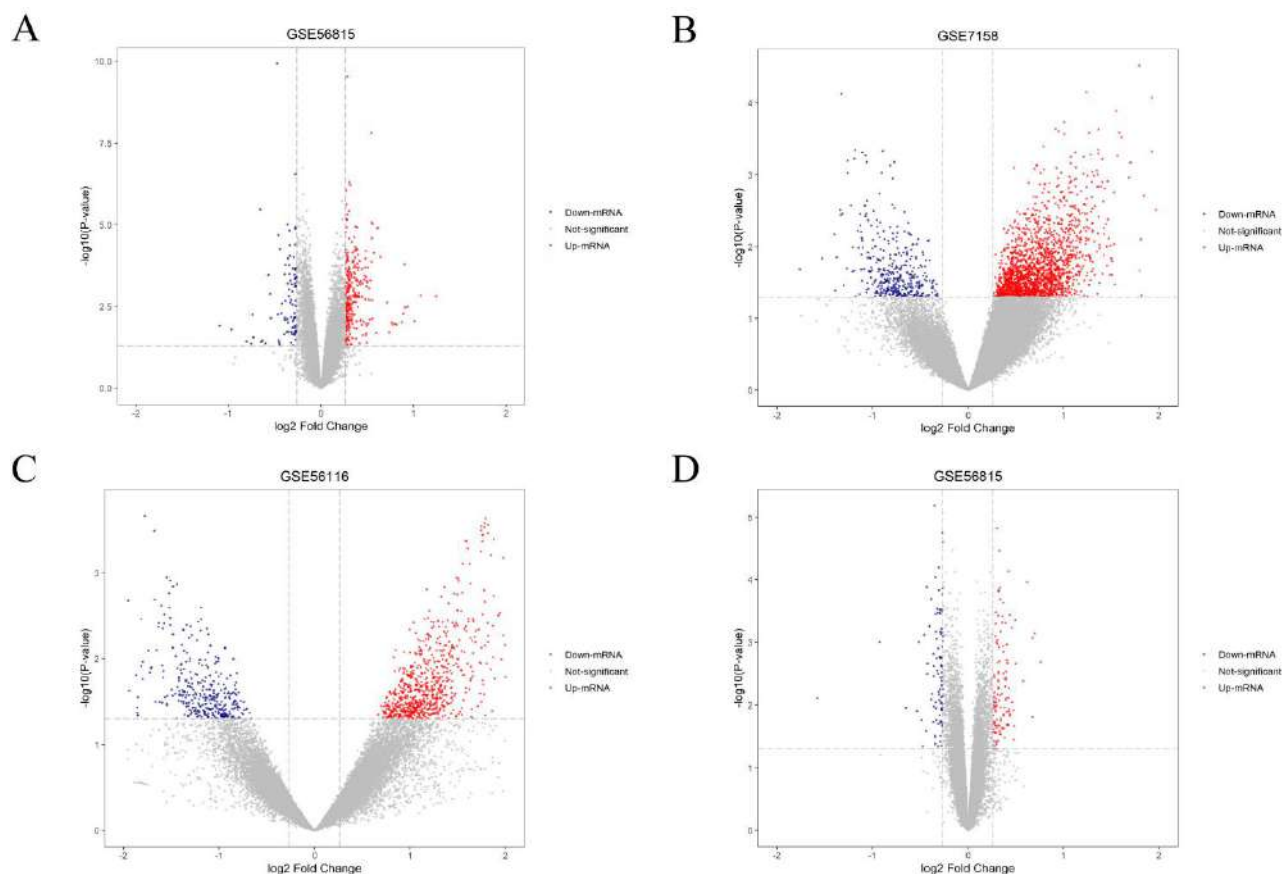
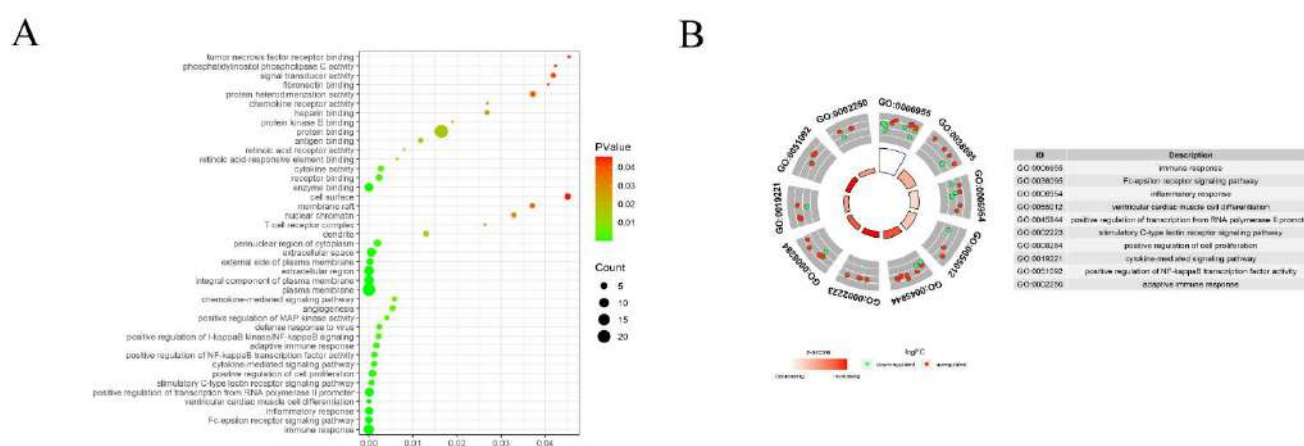
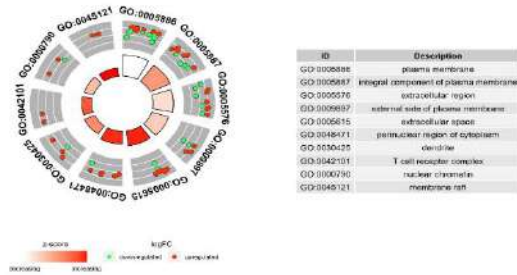


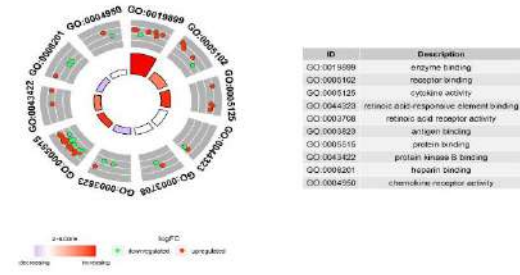
Figure 2. Osteoporosis-related differentially expressed genes (OP-DEGs). The x-axis displays the log2 Fold Change, while the y-axis shows the -log10 of the adjusted P value. Genes with increased expression and differential expression are denoted by red nodes, genes with decreased expression are represented by blue nodes, and genes with no significant alteration in expression are indicated by gray nodes.



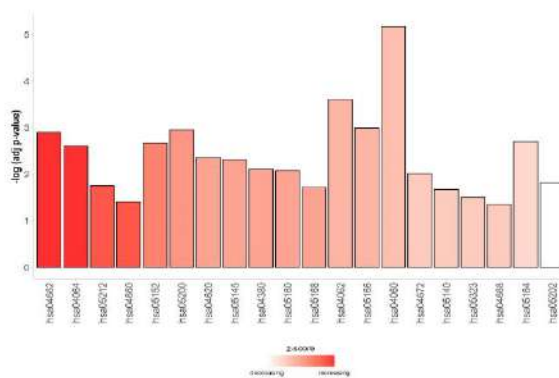
C



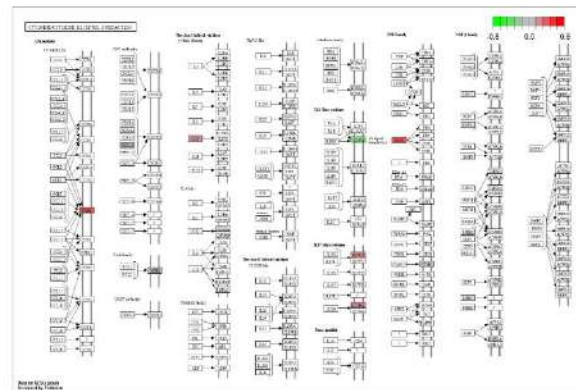
D



E



F



G

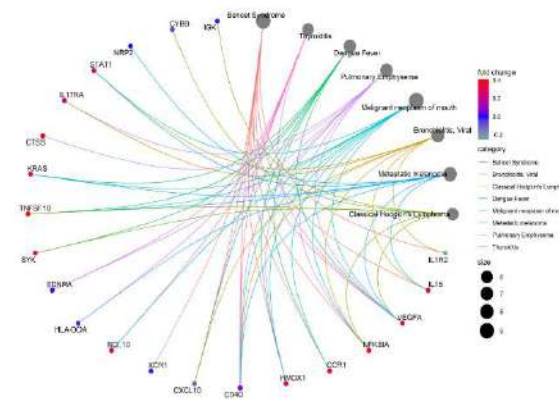


Figure 3. GO functional annotation and KEGG pathway enrichment analysis. (A) Analysis of differentially expressed genes (DEGs) enriched in Gene Ontology (GO) terms revealed the following results. The gene ratio is represented on the horizontal axis, and the GO term is displayed on the vertical axis. The color of each node denotes the p-value significance, while the size of the node corresponds to the number of genes linked to the respective GO term. (B–D) Gene expression visualization in the top 10 categories of enriched Biological Processes (BP), Cellular Components (CC), and Molecular Functions (MF) from GO analysis. The nodes' color represents the level of gene expression, with green indicating downregulation and red indicating upregulation. The color scheme of the quadrilateral shapes reflects the impact of gene expression on the GO term; red denotes activation, and white represents inhibition. (E) The OP-DEGs' results of KEGG enrichment analysis. Pathway names are shown on the horizontal axis, and significant p values are shown on the vertical axis. The columns are color-coded to indicate gene expression effects on pathways: red for activation and white for inhibition. (F) Enrichment results of cytokine-cytokine receptor interaction. (G) Disease Ontology enrichment analysis results of OP-DEGs. The color of the nodes in the network indicates the magnitude of the log₂FC, while the size of the nodes represents the number of genes associated with the disease under investigation. Additionally, the color of the lines connecting the nodes signifies the different diseases being studied.

GSEA

The relationship between gene expression and biological processes (BP), molecular functions (MF), and cellular components (CC) was examined in four datasets to determine how gene expression influences osteoporosis. Our findings indicated that genes from the GSE56815 premenopausal dataset predominantly influenced critical biological functions, including actin filament organization, immune response activation, cell-substrate junctions, and chromatin covalent modification (refer to Figures 4A–B and Supplementary Table S4). Genes in GSE7158 mostly affected biologically relevant functions such as actin-binding, actin cytoskeleton, anatomical structure homeostasis, and anion transmembrane transport (Figure 4C–D and Supplementary Table S5). GSE56116 showed numerous genes that were associated with vital biological functions, including amide binding, azurophilic granules, immune response regulation signaling pathways, and leukocyte migration (Figure 4E - F and Supplementary Table S6). Genes in GSE56815 postmenopausal data primarily affected biological relevant functions such as actin binding, actin cytoskeleton, B-cell activation, and cadherin binding (Figure 4G–H and Supplementary Table S7).

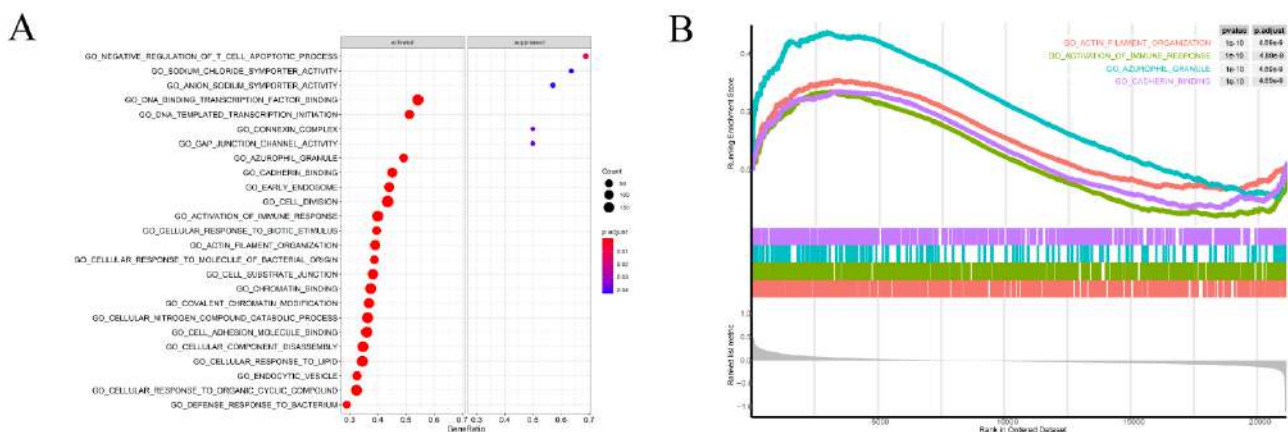
GSVA

Based on GSVA analysis of the four sample groups, along with limma differential analysis, it was observed that the following functions were prominently different between normal and OP tissues in the GSE56815

premenopausal dataset: the hallmark UV response signature, complement activation signature, peroxisome signature, and apoptosis signature (refer to Figure 6A). For GSE7518 data, the functions of hallmark UV response up, hallmark allograft rejection, hallmark peroxisome, and hallmark apoptosis differed significantly between normal tissues and OP tissues (Figure 6B). For GSE56116 data, functions of hallmark UV response up, hallmark complement, hallmark peroxisome, and hallmark apoptosis differed significantly between normal tissues and OP tissues (Figure 6C), whereas for GSE56815 postmenopausal data, these functions were hallmark UV response up and hallmark interferon alpha response (Figure 6D).

Immune Infiltration Analysis

To analyze the correlation between OP-DEGs and the degree of immune infiltration in OP tissues and normal tissues, we used the CIBERSORT algorithm to calculate the degree of 22 types of immune cell infiltration in OP tissues and normal tissues in four groups of data (Figure 7). The findings indicated that four genes had a significant association with a minimum of four types of immune cells in Data Group 1 (Figure 8A), two genes were closely related to at least four immune cells in Data Group 2, 16 genes were closely related to at least four immune cells in Data Group 3 (Figure 8B), and six genes were closely related to at least four immune cells in Data Group 4 (Figure 8C). According to the union set of the above genes, we obtained 20 key OP-related immune genes (Figure 8D).



Immune Infiltration Genes Linked to Osteoporosis Prognosis

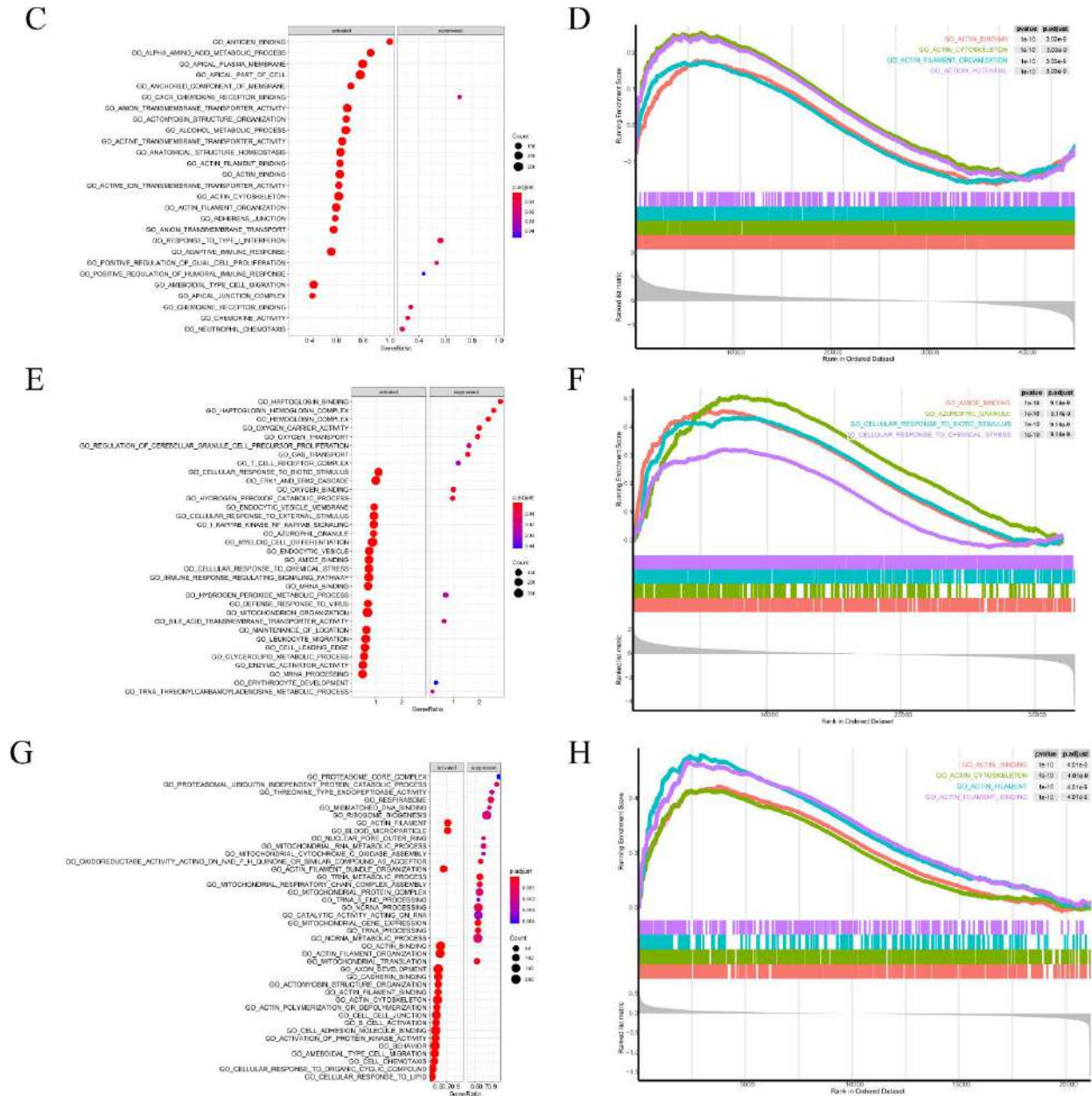
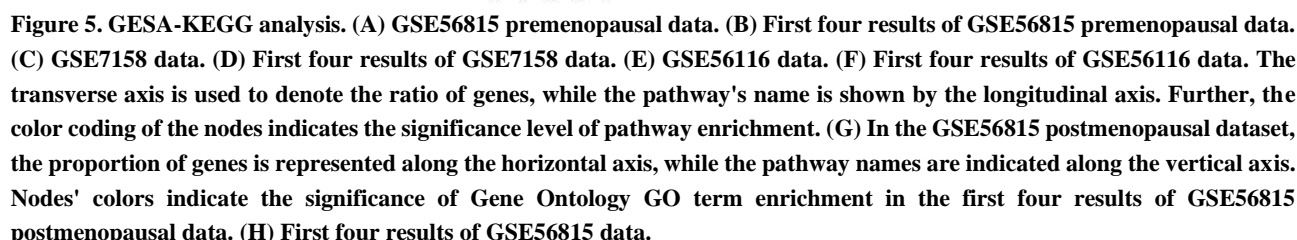


Figure 4. GSEA-GO analysis. (A) GSE56815 premenopausal data. (B) First four results of GSE56815 premenopausal data. (C) GSE7158 data. (D) First four results of GSE7158 data. (E) GSE56116 data. (F) First four results of GSE56116 data. (G) GSE56815 postmenopausal data. (H) First four results of GSE56815 postmenopausal data. On the horizontal axis are the percentages of genes, while on the vertical axis are the Gene Ontology (GO) terms. GO term enrichment is indicated by the color of each node, and the size of the node represents how many genes are associated with the term.

Moreover, Gene Set Enrichment Analysis (GSEA) on the GSE56815 premenopausal dataset indicated that gene expression is primarily associated with Huntington's disease, cancer-related pathways, chemokine signaling, and Soluble N-ethylmaleimide-sensitive factor Attachment protein REceptor (SNARE) involvement in vesicle trafficking (refer to Figure 5A–B). For GSE7518, gene expression was mainly related to the calcium signaling pathway, Wnt signaling pathway, ECM receptor interaction, and hedgehog signaling pathway (Figure 5C–D). For GSE56116, gene expression was mainly related to leishmania infection, pathways in cancer, the chemokine signaling pathway, and glycerolipid metabolism (Figure 5E–F). As shown in Figure 5G–H, GSEA analysis of the postmenopausal data from GSE56815 revealed a strong association between gene expression and focal adhesions, MAPK signaling, and tight junctions.



Immune Infiltration Genes Linked to Osteoporosis Prognosis

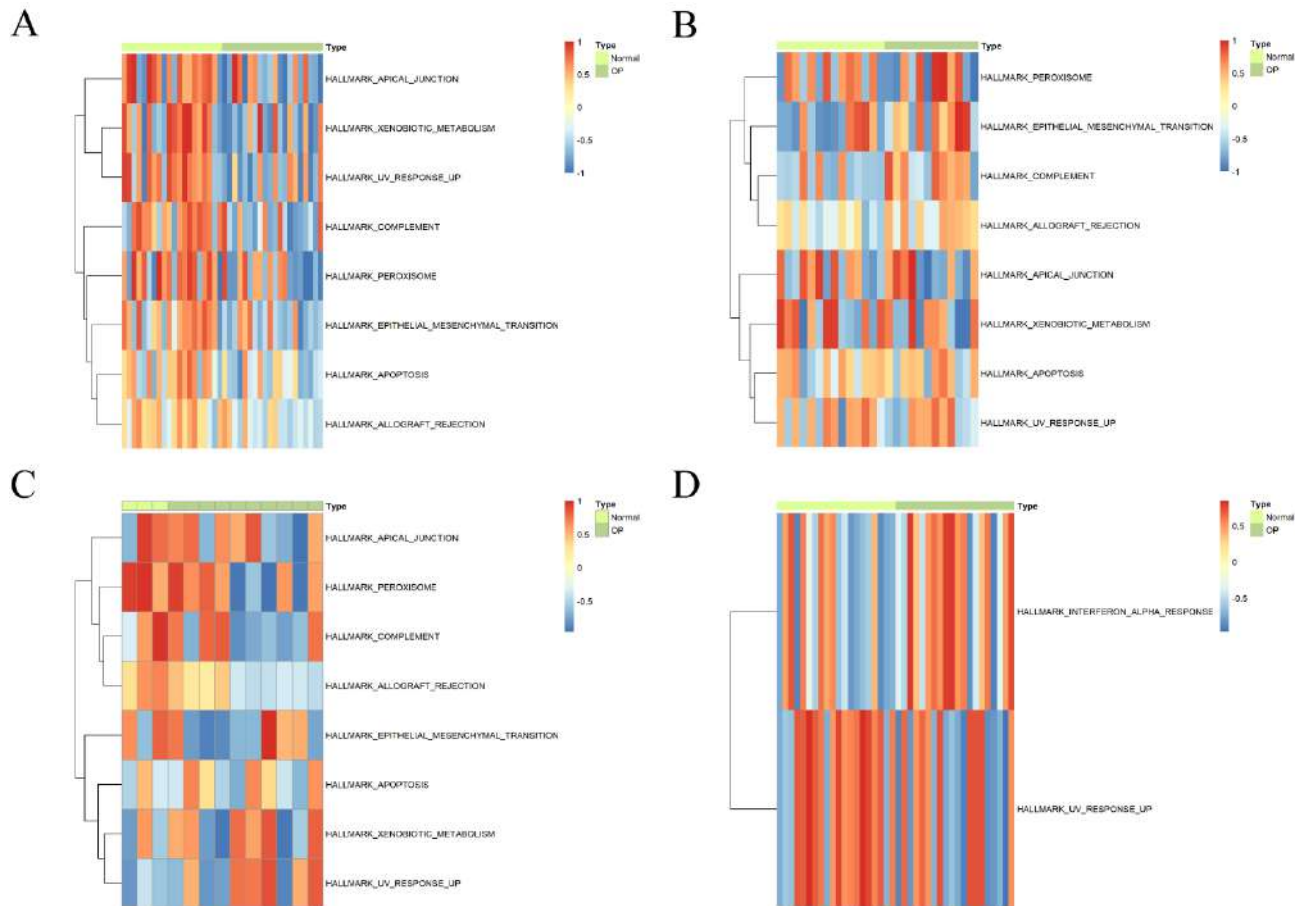


Figure 6. GSVA analysis. (A) GSE56815 premenopausal data. (B) GSE7158 data. (C) GSE56116 data. (D) GSE56815 postmenopausal data. Nodes are colored by Hallmark enrichment scores, with the horizontal axis representing patient identification, the vertical axis representing hallmark gene sets, and the horizontal axis representing patient identification.

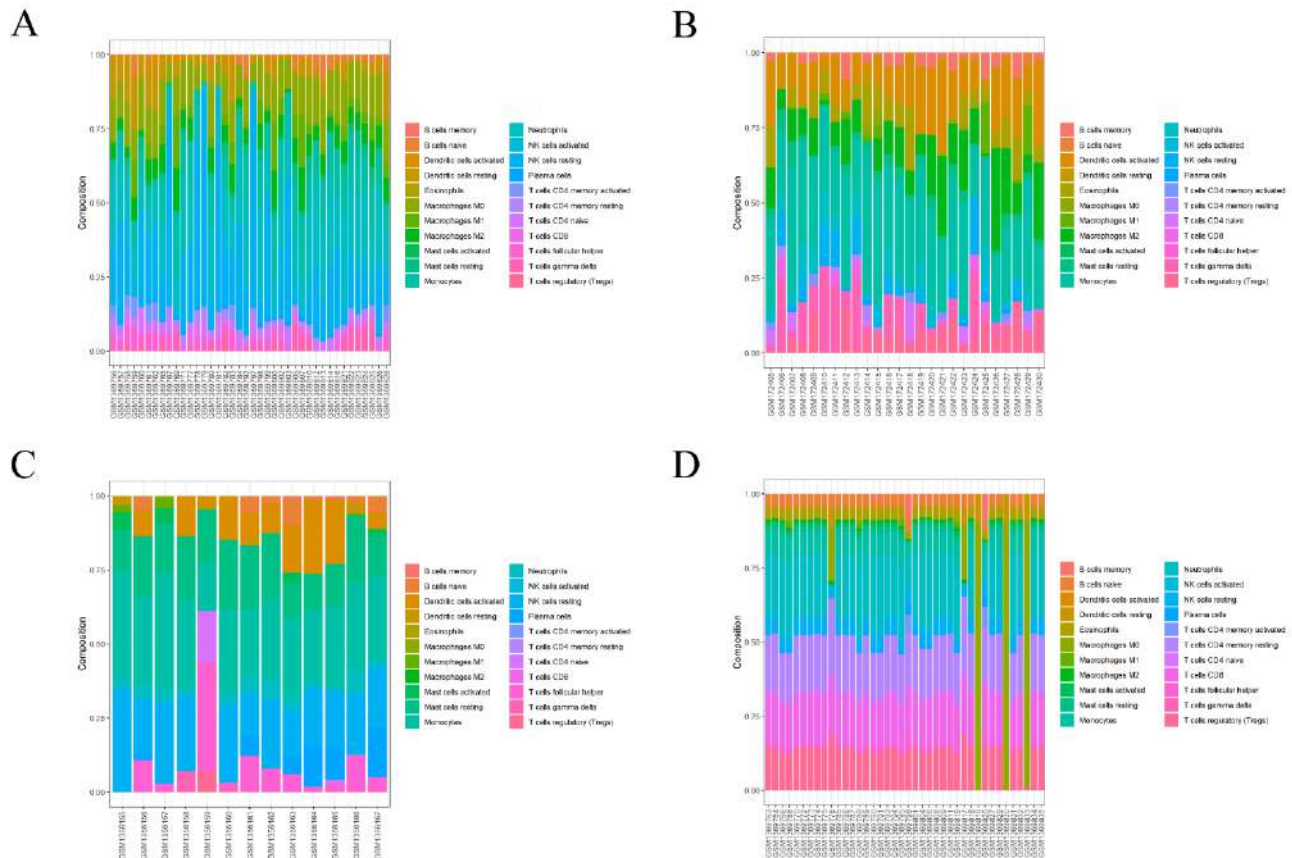


Figure 7. Immune infiltration analysis. (A) GSE56815 premenopausal data. (B) GSE7158 data. (C) GSE56116 data. (D) GSE56815 postmenopausal data. The vertical axis indicates the percentage of immune cells, and the horizontal axis indicates patient ID. Node color represents the different immune cells.

Immune Infiltration Genes Linked to Osteoporosis Prognosis

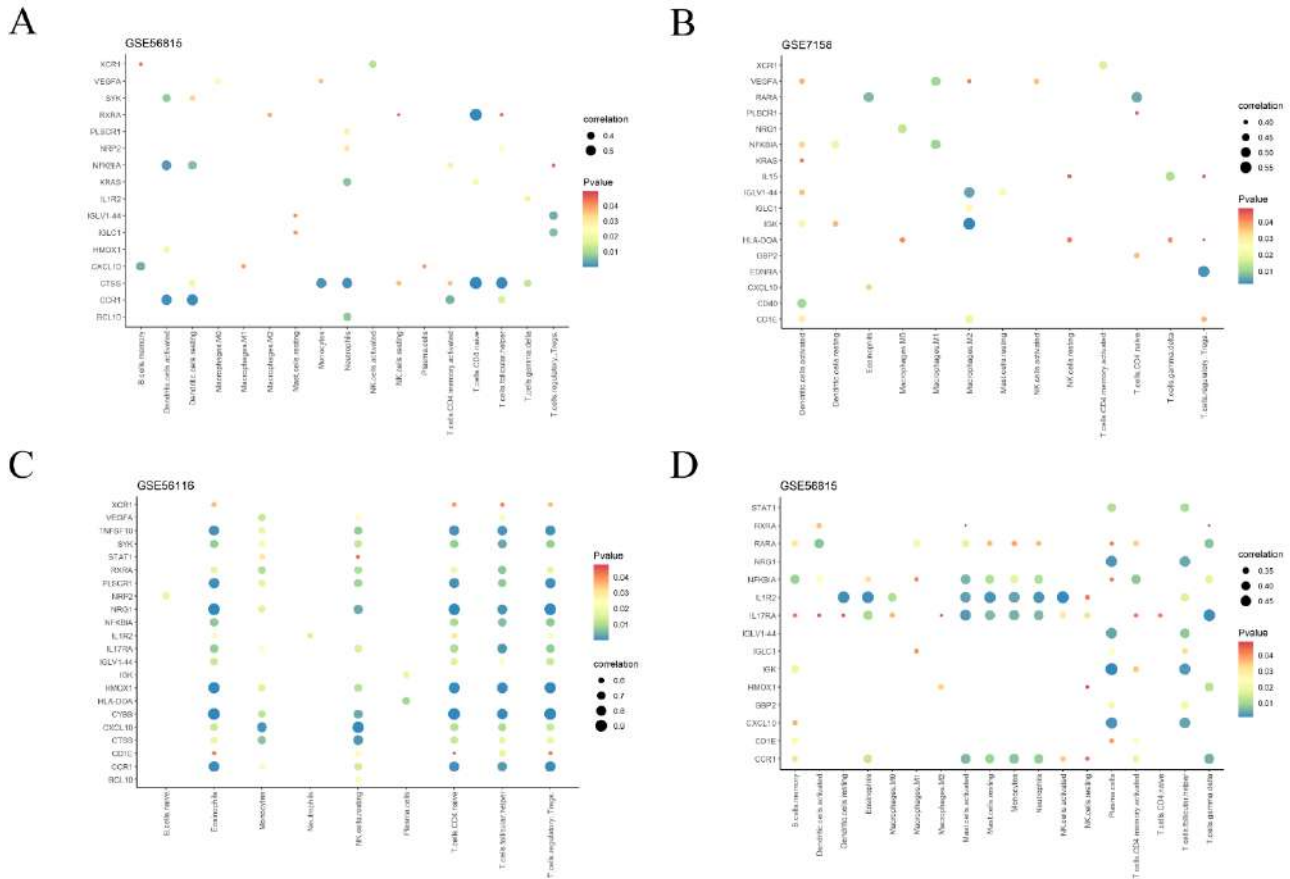


Figure 8. Key osteoporosis-related immune genes. (A) GSE56815 premenopausal data. (B) GSE7158 data. (C) GSE56116 data. (D) GSE56815 postmenopausal data. These plots display the correlation between Osteoporosis-related differentially expressed genes (OP-DEGs) and immune cells in osteoporotic and normal tissues. The horizontal axis represents the immune cells, while the vertical axis represents the OP-DEGs. The significance of correlations is denoted by node color, while their absolute values are suggested by node size.

The Competitive Endogenous RNA Network Involving Key Immune Genes Related to Osteoporosis.

We constructed a ceRNA network of key OP-related immune genes, which contained 18 mRNAs, 603 miRNAs, and 11,213 lncRNAs (Figure 9A). The top five targeting key OP-related immune genes of miRNA were *VEGFA* regulated by 207 miRNAs, *PLSCR1* regulated by 94 miRNAs, *HMOX1* regulated by 78 miRNAs, *RARA* regulated by 58 miRNAs, and *CXCL10* regulated by 55 miRNAs. The top five miRNAs that simultaneously controlled multiple key immune genes related to osteoporosis included *hsa-mir-124-3p*, *hsa-mir-20a-5p*, and *hsa-mir-34a-5p*, which regulated seven key osteoporosis-related immune genes, along with *hsa-mir-128-3p* and *hsa-mir-129-2-3p*, which regulated six key osteoporosis-related immune genes. The top five

lncRNAs with the most binding relationships to miRNAs in the network were *NEAT1* (binding to 204 miRNAs), *KCNQ1OT1* (binding to 203 miRNAs), *XIST* (binding to 186 miRNAs), *OIP5-AS1* (binding to 112 miRNAs), and *HCG18* (binding to 107 miRNAs), whereas the top five miRNAs with the most associations with lncRNAs were *hsa-mir-15a-5p*, *hsa-mir-15b-5p* (binding to 114 lncRNAs), *hsa-mir-6838-5p* (binding to 113 lncRNAs), and *hsa-mir-16-5p* and *hsa-mir-195-5p* (binding to 112 lncRNAs). Furthermore, 243 miRNAs exhibited a regulatory nexus with both key OP-related immune genes and lncRNAs (Figure 9C); for example, *hsa-mir-296-5p*, *hsa-mir-30e-5p*, and *hsa-mir-361-5p2* (Figure 9B,9D).

Validation of Key Osteoporosis-related Immune Genes

We first corrected the data (Figure 10A–B) and analyzed the correlation between OP-DEGs and the

degree of immune infiltration in OP tissues compared to normal tissues. Within the validation dataset, the CIBERSORT method was employed to quantify the infiltration levels of 22 immune cell types in both OP and normal tissues (Figure 10C). Subsequently, the

associations between 20 crucial OP-associated immune genes and these immune cells were determined. The results showed that 14 genes were closely related to 13 immune cells (Figure 10D).

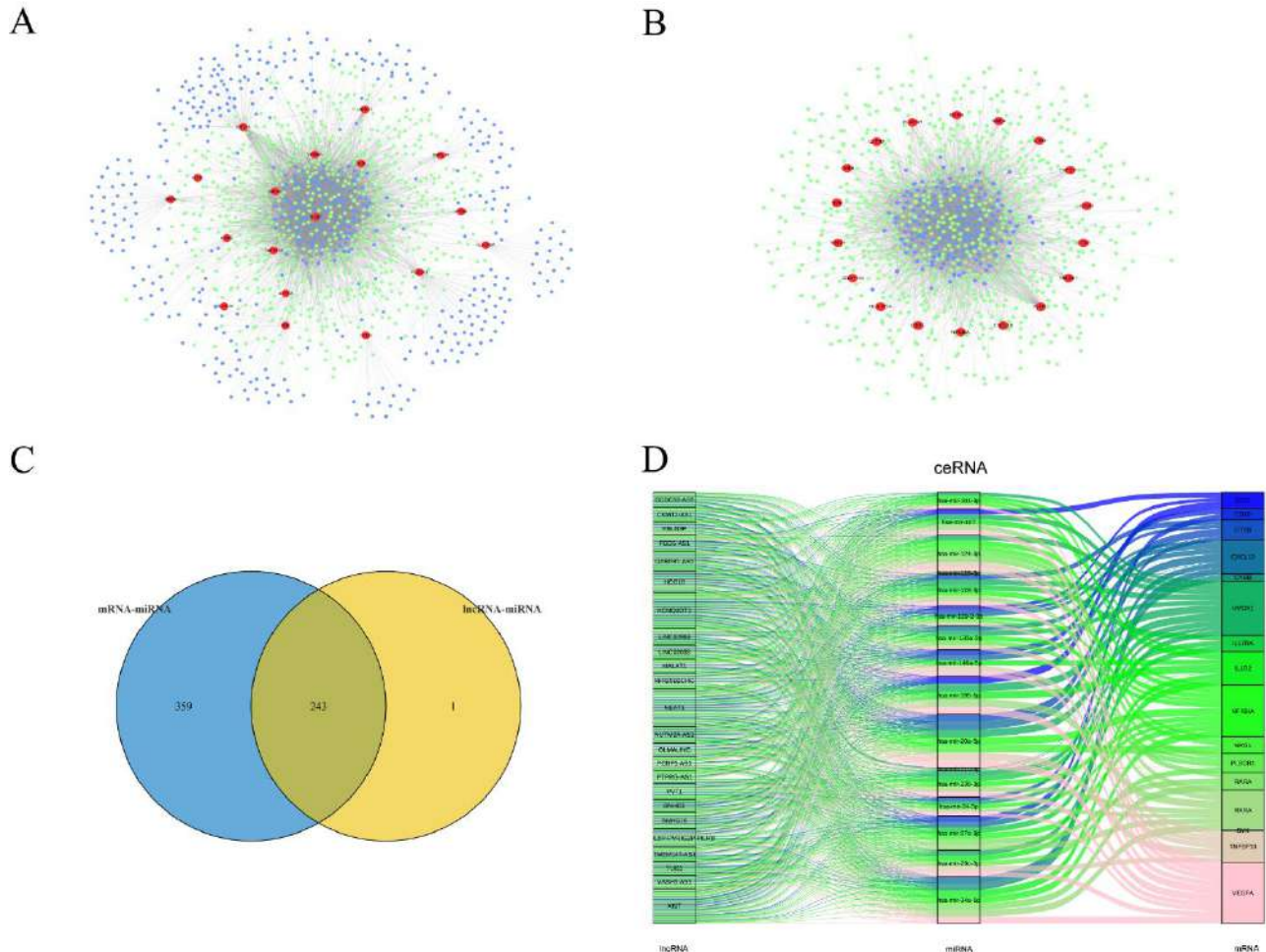


Figure 9. CeRNA network. (A) ceRNA network of key osteoporosis-related immune genes. (B) miRNA-related ceRNA networks displayed a regulatory relationship with both key osteoporosis-related immune genes and lncRNAs. Red nodes are key osteoporosis-related immune genes, blue nodes are miRNAs regulating the key osteoporosis-related immune genes, and green nodes are the lncRNAs. (C) miRNAs displaying a regulatory relationship with both key osteoporosis-related immune genes and lncRNAs. (D) The Sankey plot of the ceRNA network.

Immune Infiltration Genes Linked to Osteoporosis Prognosis

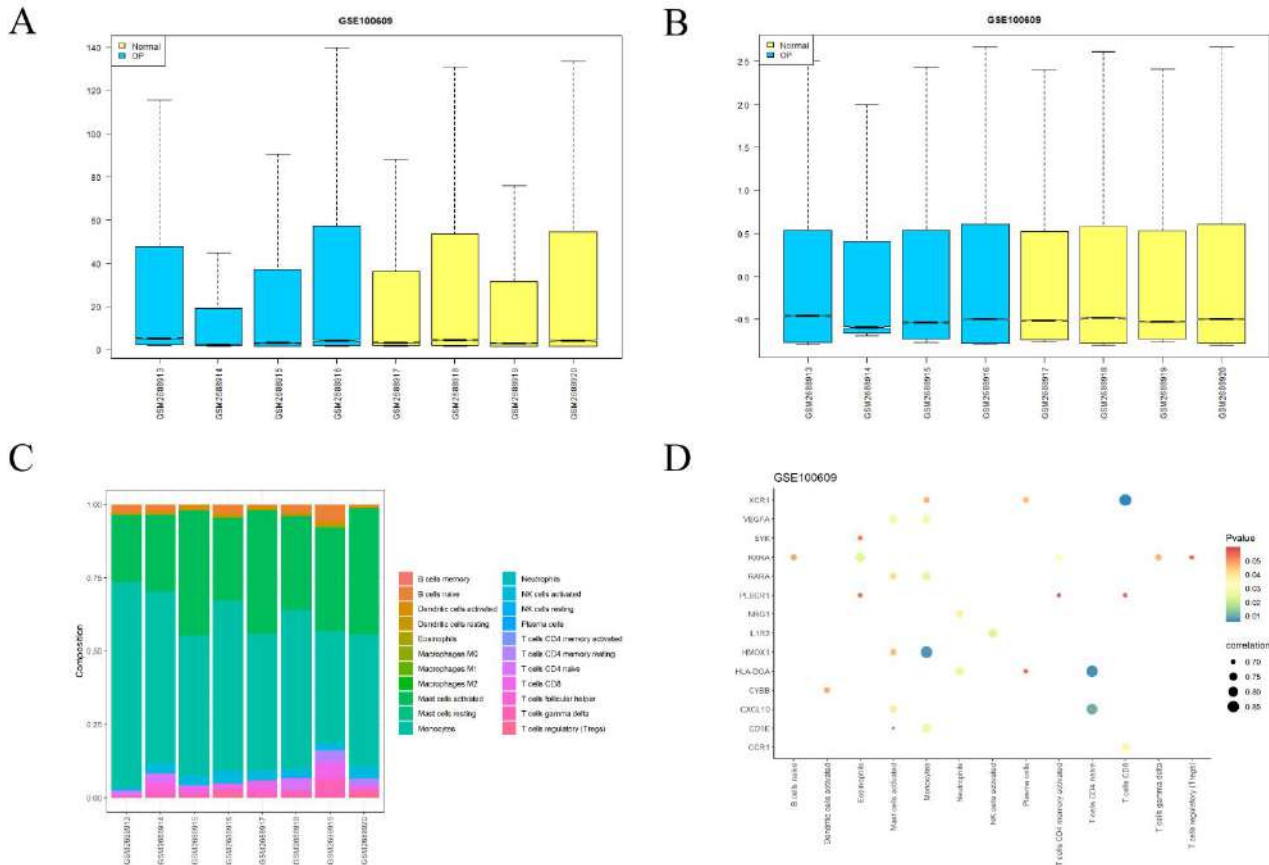


Figure 10. Validation of GSE100609 data. (A–B) Correction of osteoporosis-related data. Abscissa is the patient ID, ordinate is the gene expression level, blue indicates osteoporosis tissue, and yellow indicates normal tissue. A represents pre-correction data, and B represents corrected data. (C) Immune infiltration analysis of GSE100609 data. A transverse axis indicates the patient's ID, and a longitudinal axis indicates the proportion of immune cells. Node color represents the different immune cells. (D) Correlation between key osteoporosis-related immune genes and immune cells in osteoporotic and normal tissues in GSE100609 data. The transverse axis indicates immune cells and the longitudinal axis indicates key osteoporosis-related immune genes. The correlation's significance is indicated by the color of the nodes, and their absolute values are conveyed through the nodes' size.

Diagnostic Efficacy Analysis of Key Osteoporosis-Related Immune Genes

To further analyze the influence of key OP-related immune genes on OP diagnosis, we drew the ROC curves for 20 key OP-related immune genes in five datasets and then calculated the AUC values (Figure 11). In the analysis of five distinct datasets, immune genes linked to OP and possessing an AUC value exceeding 0.5 were deemed to have prognostic significance. As a result, we identified 11 key OP-related immune genes with prognostic value, including *CD1E*, *CYBB*, *HMOX1*, *GLV1-44*, *IL17RA*, *IL1R2*, *NRG1*, *PLSCR1*, *SYK*, *TNFSF10* and *IGK*.

The Experiment on 15 Key Osteoporosis-related Immune Genes

Subsequently, we assessed the expression levels of 15 crucial OP-associated immune genes in both OP and normal control groups using RT-PCR. In Supplementary Table S8, primers for RT-PCR are listed. The RT-PCR analysis shows a decrease in the mRNA levels of *hsa-mir-34a-5p* and *hsa-mir-128-3p* in OP compared to controls, but no significant differences were found. In contrast, the reverse findings were noted for the remaining 13 genes. Besides, the gene expression of *VEGFA*, *HMOX1*, *RARA*, *CXCL10*, *hsa-mir-129-2-3p*, *OIP5-AS1*, and *HCG18* increased significantly ($p < 0.05$).

In addition, no significant differences were observed between the OP group and control group in the levels of

PLSCR1, *hsa-mir-124-3p*, and *hsa-mir-20a-5p*, *NEAT1*, *KCNQ1OT1*, and *XIST* (Figure 12).

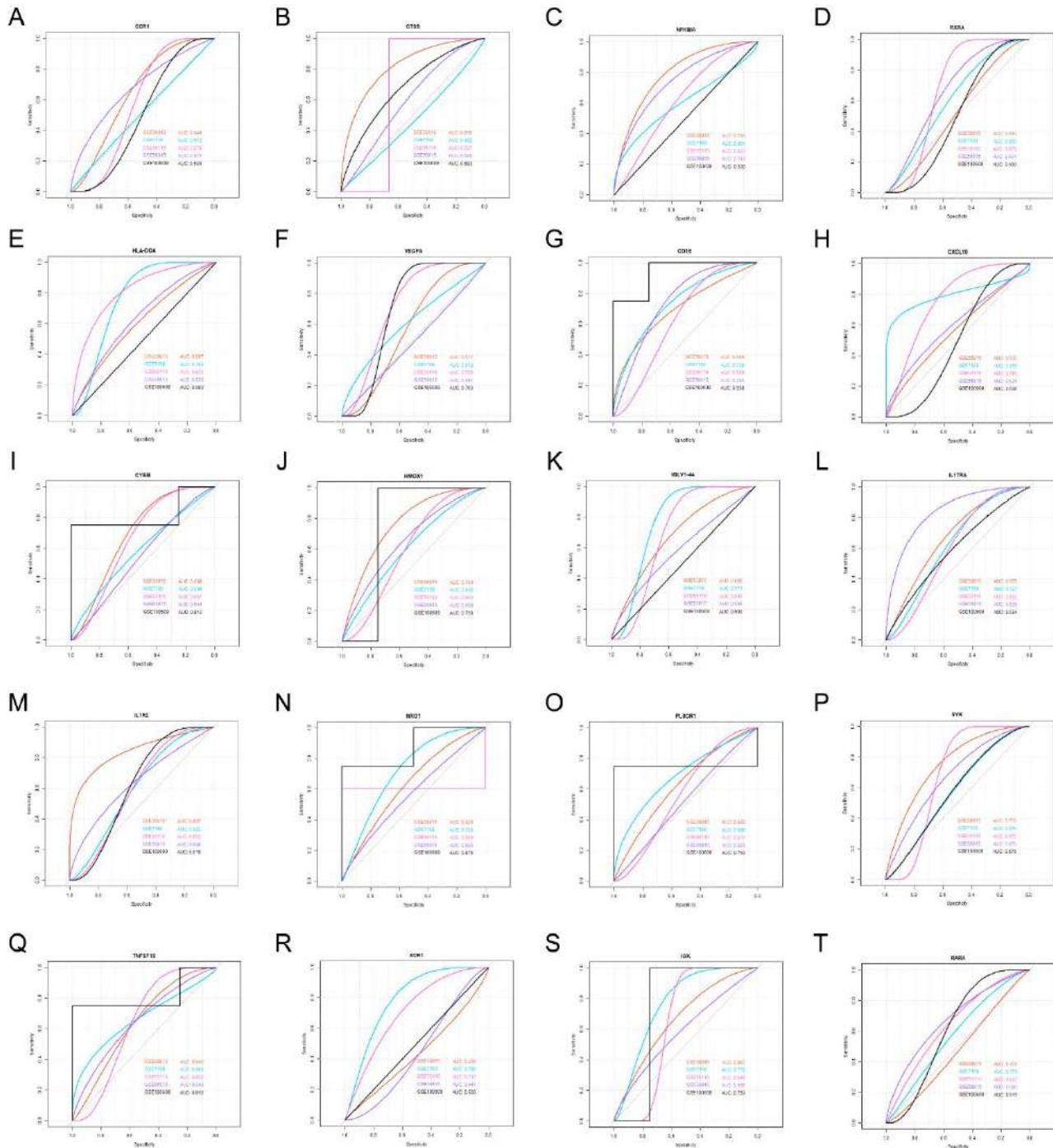


Figure 11. Diagnosis ROC curve for key osteoporosis-related immune genes. The transverse axis indicates the specificity of the test, the longitudinal axis indicates the sensitivity and the five lines represent the five respective data sets.

Immune Infiltration Genes Linked to Osteoporosis Prognosis

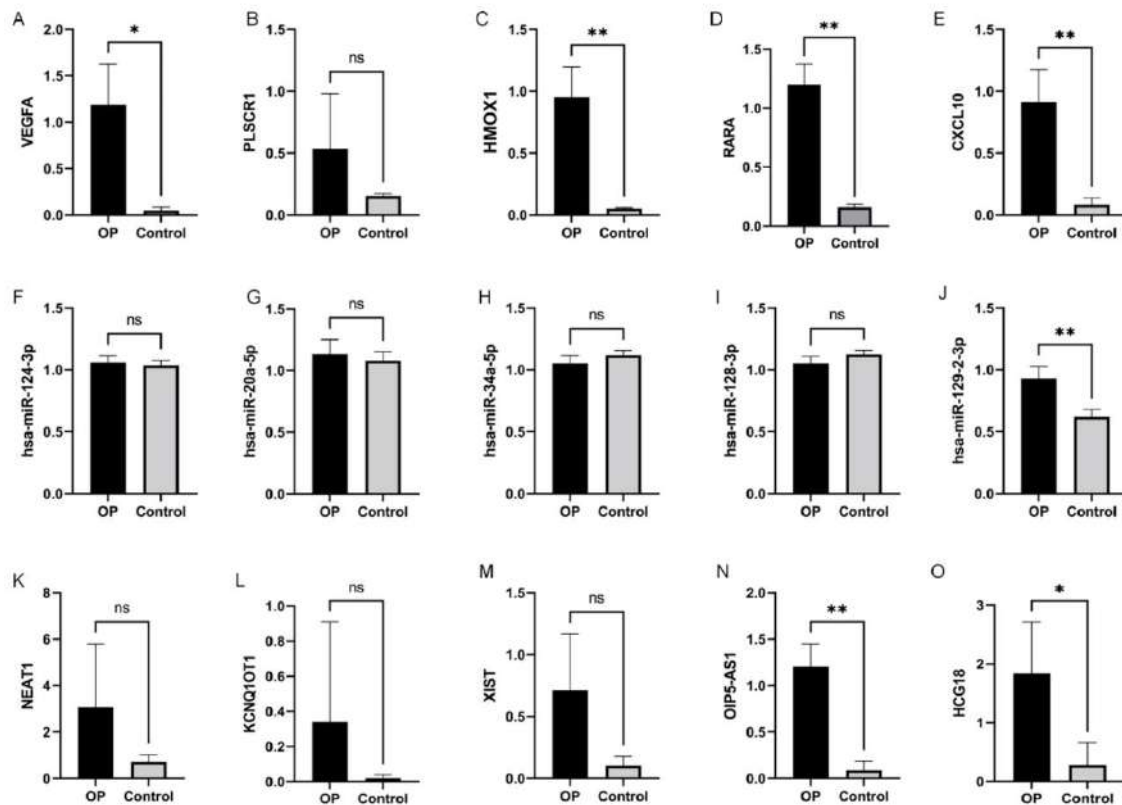


Figure 12. The qRT-PCR results of 15 key osteoporosis-related immune genes. (A-O) *VEGFA*, *PLSCR1*, *HMOX1*, *CXCL10*, *hsa-miR-124-3p*, *hsa-miR-20a-5p*, *hsa-miR-34a-5p*, *hsa-miR-128-3p*, *hsa-miR-129-2-3p*, *NEAT1*, *KCNQ10T1*, *SIXT*, *OIP5-AS1*, *HCG18*, and *RARA*.

DISCUSSION

Osteoporosis, the most prevalent bone condition, has serious implications. Prior research has demonstrated a correlation between the increasing incidence of osteoporosis, the inadequacies of existing treatment modalities, and the persistent occurrence of reduced bone density and osteoporotic fractures, underscoring the necessity of understanding the underlying mechanism. Despite advances in treatment strategies, no effective therapeutic targets are currently available for OP, and no sensitive biomarkers have yet been identified for the diagnosis and prevention of OP. Furthermore, the close relationship between the immune system and bone metabolism, as well as the potential impact of interactions between bone cells and immune cells on the development of OP, have been highlighted.

Consequently, we conducted a thorough bioinformatics investigation into OP utilizing four gene expression datasets to pinpoint potential biomarkers.²⁹

OP-DEGs, which consist of immune-related genes, were discovered. Functional annotations using GO analysis indicated that these OP-DEGs were predominantly involved in immune response, plasma membrane functions, and enzyme binding. Analysis via the KEGG pathway revealed that the interaction between cytokines and their receptors was of utmost significance. GSEA and GSVA analyses showed that enriched pathways and modules were linked to immune response and genes upregulated in response to UV radiation. In addition,²⁰ key immune genes related to OP, which were identified by immune infiltration analysis, demonstrated high diagnostic potential for OP.

By constructing a ceRNA network of key OP-related immune genes, we have identified the top 5 miRNAs that target these critical immune genes as well as the top 5 miRNAs that control multiple OP-related immune genes. Additionally, we have discovered the top 5 lncRNAs within this network that interact most frequently with miRNAs, along with the top 5 miRNAs

that have the most interactions with lncRNAs. Our research found that 11 key genes associated with OP had prognostic value. To validate our bioinformatic results, we performed RT-PCR on our OP patient samples for a total of 15 selected genes. A significant increase in mRNA levels of *VEGFA*, *HMOX1*, *RARA*, *CXCL10*, *hsa-mir-129-2-3p*, *OIP5-AS1*, and *HCG18* was noted in osteoporosis patients compared to controls. For example, *HMOX1* (heme oxygenase), not only plays a role in reducing fat differentiation in fat metabolism but also enhances bone differentiation in bone development.⁴⁵ Additionally, *HMOX1* can play an anti-adsorption role in the pathogenesis of OP and reduce bone loss by blocking bone differentiation.⁴⁶ This means that *HMOX1* contributes to combating the reduction in bone mass that occurs with aging. Increasing *HMOX1* expression can also reduce the level of intracellular reactive oxygen species, which could affect the balance between bone resorption and bone formation, thereby alleviating OP.⁴⁷ *HMOX1* could serve as a promising therapeutic target for OP prevention. Research has indicated that *VEGFA* is a significant factor within the context of OP. *VEGFA*, an angiogenic factor, is induced in human mesenchymal stem cells and human adipose-derived stem cells from osteoporotic donors in response to uniaxial cyclic tensile strain.⁴⁸ This suggests that down-regulating *VEGFA* expression can suppress osteogenic differentiation, making it a potential therapeutic target for OP.⁴⁹ This suggestion is supported by our findings.

Analysis of GO and KEGG for the 29 OP-DEGs revealed their predominant enrichment in immune response, plasma membrane, and enzyme binding categories. Among the pathways studied, cytokine-cytokine receptor interaction was the most prominent. In individuals with OP, defining traits include reduced bone density and compromised microarchitecture.⁵⁰ Research indicates that the immune response, known for its significant influence on bone metabolism, could be crucial in the advancement of osteoporosis (OP).^{51,52} Similarly, our study revealed that OP-DEGs and immune response were indeed correlated.

Moreover, emerging research has provided new evidence that membrane trafficking in osteoclasts may be exploited for the development of new therapies for metabolic bone disorders such as OP.⁵³ As a result, these differentially expressed genes are closely related to the onset and progression of OP.

DEGs linked to OP were further analyzed using GSVA and GSEA. Actin filament organization, actin

binding, and amide binding were the three main enriched biological functions in the three diverse datasets. Huntington's disease, the calcium signaling pathway, lysosome, and focal adhesion were the four major pathways among these datasets. GSVA analysis revealed a significant differential expression of the hallmark UV response in genes across these datasets. Actin and UV significantly enriched biological functions. Notably, osteoclasts feature an exceptionally dynamic actin cytoskeleton that is crucial for their role in bone resorption.⁵⁴ Previous research has shown that an inhibitor of the binding interaction, which is engaged by the actin cytoskeleton, blocks bone resorption in pre-clinical animal models, including a model of postmenopausal OP.⁵⁵ In addition, short-range UV irradiation may ameliorate postmenopausal OP associated with vitamin D deficiency.⁵⁶ Furthermore, irradiation with UV-LED (305 nm) increases vitamin D production, bone density, and strength.⁵⁷

Through immune infiltration analysis and diagnostic efficacy analysis, we identified 11 key OP-related immune genes with prognostic value. These genes are *CD1E*, *CYBB*, *HMOX1*, *GLV1-44*, *IL17RA*, *IL1R2*, *NRG1*, *PLSCR1*, *SYK*, *TNFSF10*, and *IGK*. Several previous studies have also reported key OP genes that could be used as potential biomarkers. *CD1E* is the only gene stored in soluble form in human CD1 protein in the late endophytes of dendritic cells, which can present lipid or glycolipid antigens.⁵⁸ Research demonstrates an association between reduced bone mineral density in OP sufferers and an increase in marrow adiposity.⁵⁹ Additionally, elevated levels of high-density lipoproteins are observed in the blood of those with OP,⁶⁰ implying a possible role of lipids in OP's development. *CD1E* may also serve as a promising osteoporosis biomarker, according to our study. *SYK* (spleen tyrosine kinase) plays a crucial role in adaptive immune receptor signaling,⁶¹ which is predominantly involved in the signal transmission of various immune sensors. Currently, bone marrow cells lacking *SYK* struggle to develop into OP.⁶²⁻⁶⁴ Our results suggest that the development of drugs inhibiting *SYK* expression could benefit the treatment of OP.

However, there are limitations to this research. Firstly, additional validation through animal studies was not conducted. Many biomarkers linked to OP have yet to be fully identified, necessitating further analysis and experimental validation to ascertain the significance of these crucial genes in the context of OP. Secondly, due to

the lack of corresponding clinical correlation research, we were not able to analyze the results in combination with clinical information. Finally, the large number of datasets may have resulted in inter-batch differences that could not be avoided or removed during analysis.

In summary, this investigation delved into the molecular processes underlying the progression and prevention of OP. Utilizing extensive bioinformatics methods and qRT-PCR, we pinpointed crucial immune genes linked to OP as potential biomarkers. Nonetheless, the precise pathogenic pathways and molecular targets require additional validation.

STATEMENT OF ETHICS

The Ethics Committee of Guangzhou Red Cross Hospital approved this research (approval number:2023-126-01). It followed the ethical guidelines outlined in the 1964 Helsinki Declaration and subsequent amendments or comparable standards.

FUNDING

This study was supported by funding from various sources, including the General Guiding Project of Guangzhou Health and Medical Science and Technology (Grant Number 2024A010017), the Teaching Reform Research Project of Guangdong Provincial Clinical Teaching Base (Grant Number 2021JD196), the 2024 Joint Municipal-University(Hospital)-Enterprise Funding Program of Guangzhou Science and Technology Bureau (Grant Numbers 2023A03J0987,2024A03J0594), the Innovation and Entrepreneurship Training Program for University Students (Grant Numbers 20221573056,202310573043), and the Clinical Frontier Technology Program of the First Affiliated Hospital of Jinan University, China. JNU1AF-CFTP-2022-a01204).

CONFLICT OF INTEREST

The authors declare no conflicts of interest.

ACKNOWLEDGMENTS

The authors would like to thank the staff of Jinan University and the Department of Orthopedics and Nursing Department of the Guangzhou Red Cross

Hospital of Jinan University for their financial support of this research.

DATA AVAILABILITY

The data for this study can be accessed from the corresponding author upon a reasonable request.

REFERENCES

1. Hernlund E, Svedbom A, Ivergard M, Compston J, Cooper C, Stenmark J, et al. Osteoporosis in the European Union: medical management, epidemiology and economic burden. A report prepared in collaboration with the International Osteoporosis Foundation (IOF) and the European Federation of Pharmaceutical Industry Associations (EFPIA). *Arch Osteoporos*. 2013;8(1):136.
2. Cheng X, Zhao K, Zha X, Du X, Li Y, Chen S, et al. Opportunistic Screening Using Low-Dose CT and the Prevalence of Osteoporosis in China: A Nationwide, Multicenter Study. *J Bone Miner Res*. 2021;36(3):427-35.
3. Compston JE, McClung MR, Leslie WD. Osteoporosis. *Lancet*. 2019;393(10169):364-76.
4. Yang J, Tang Q, Che M, Shi J, Yang L, Zeng Y. Effect of bedside health education for elderly patients with fragility fracture by specialist physicians on the diagnosis and treatment of osteoporosis during hospitalization and the visiting rate to osteoporosis clinic after discharge in a high-volume orthopedic hospital. *Arch Osteoporos*. 2023;18(1):133.
5. Matsumoto T, Endo I. RANKL as a target for the treatment of osteoporosis. *J Bone Miner Metab*. 2021;39(1):91-105.
6. Katoh M, Katoh M. Molecular genetics and targeted therapy of WNT-related human diseases (Review). *Int J Mol Med*. 2017;40(3):587-606.
7. De Martinis M, Sirufo MM, Ginaldi L. Osteoporosis: Current and Emerging Therapies Targeted to Immunological Checkpoints. *Curr Med Chem*. 2020;27(37):6356-72.
8. Zhao W, Wang G, Zhou C, Zhao Q. The regulatory roles of long noncoding RNAs in osteoporosis. *American Journal of Translational Research*. 2020. 12(9): 5882-5907.
9. Ohnishi T, Ogawa Y, Suda K, Komatsu M, Harmon SM, Asukai M, et al. Molecular Targeted Therapy for the Bone Loss Secondary to Pyogenic Spondylodiscitis Using Medications for Osteoporosis: A Literature Review. *Int J Mol Sci*. 2021;22(9):4453.
10. Ukon Y, Makino T, Kodama J, Tsukazaki H, Tateiwa D,

- Yoshikawa H, et al. Molecular-Based Treatment Strategies for Osteoporosis: A Literature Review. *Int J Mol Sci*. 2019;20(10):2557.
11. Eastell R, Szulc P. Use of bone turnover markers in postmenopausal osteoporosis. *Lancet Diabetes Endo*. 2017;5(11):908-23.
12. Ciuffi S, Donati S, Marini F, Palmini G, Luzi E, Brandi ML. Circulating MicroRNAs as Novel Biomarkers for Osteoporosis and Fragility Fracture Risk: Is There a Use in Assessment Risk? *Int J Mol Sci*. 2020;21(18):6927.
13. Garnero P. The Utility of Biomarkers in Osteoporosis Management. *Mol Diagn Ther*. 2017. 21(4): 401-418.
14. Guder C, Gravius S, Burger C, Wirtz DC, Schildberg FA. Osteoimmunology: A Current Update of the Interplay Between Bone and the Immune System. *Front Immunol*. 2020;11:58.
15. Fischer V, Haffner-Luntzer M. Interaction between bone and immune cells: Implications for postmenopausal osteoporosis. *Semin Cell Dev Biol*. 2022;123:14-21.
16. Ma M, Luo S, Chen X, Yuan F, Cai J, Lu L, et al. Immune system-related differentially expressed genes, transcription factors and microRNAs in post-menopausal females with osteopenia. *Scand J Immunol*. 2015;81(3):214-20.
17. Ma M, Luo S, Zhou W, Lu L, Cai J, Yuan F, et al. Bioinformatics analysis of gene expression profiles in B cells of postmenopausal osteoporosis patients. *Taiwan J Obstet Gynec*. 2017;56(2):165-70.
18. Hu B, Kong X, Li L, Dai F, Zhang Q, Shi R. Integrative Analyses of Genes Associated with Osteoporosis in CD16+ Monocyte. *Front Endocrinol*. 2020;11:581878.
19. Ma J, Lin X, Chen C, Li S, Zhang S, Chen Z, et al. Circulating miR-181c-5p and miR-497-5p Are Potential Biomarkers for Prognosis and Diagnosis of Osteoporosis. *J Clin Endocr Metab*. 2020;105(5):dgz300.
20. Wei Y, Ma H, Zhou H, Yin H, Yang J, Song Y, et al. miR-424-5p shuttled by bone marrow stem cells-derived exosomes attenuates osteogenesis via regulating WIF1-mediated Wnt/beta-catenin axis. *Aging (Albany NY)*. 2021;13(13):17190-201.
21. Chen B, Yang W, Zhao H, Liu K, Deng A, Zhang G, et al. Abnormal expression of miR-135b-5p in bone tissue of patients with osteoporosis and its role and mechanism in osteoporosis progression. *Exp Ther Med*. 2020;19(2):1042-50.
22. Yao S, Guo Y, Dong SS, Hao RH, Chen XF, Chen YX, et al. Regulatory element-based prediction identifies new susceptibility regulatory variants for osteoporosis. *Hum Genet*. 2017;136(8):963-74.
23. Yang TL, Shen H, Liu A, Dong SS, Zhang L, Deng FY, et al. A road map for understanding molecular and genetic determinants of osteoporosis. *Nat Rev Endocrinol*. 2020;16(2):91-103.
24. Zhou Y, Gao Y, Xu C, Shen H, Tian Q, Deng HW. A novel approach for correction of crosstalk effects in pathway analysis and its application in osteoporosis research. *Sci Rep-Uk*. 2018;8(1):668.
25. Li L, Yang M, Jin A. COL3A1, COL6A3, and SERPINH1 Are Related to Glucocorticoid-Induced Osteoporosis Occurrence According to Integrated Bioinformatics Analysis. *Med Sci Monitor*. 2020;26:e925474.
26. Zhang X, Chen K, Chen X, Kourkoumelis N, Li G, Wang B, et al. Integrative Analysis of Genomics and Transcriptome Data to Identify Regulation Networks in Female Osteoporosis. *Front Genet*. 2020;11:600097.
27. Barrett T, Troup DB, Wilhite SE, Ledoux P, Rudnev D, Evangelista C, et al. NCBI GEO: mining tens of millions of expression profiles--database and tools update. *Nucleic Acids Res*. 2007;35(Database issue):D760-5.
28. Davis S, Meltzer PS. GEOquery: a bridge between the Gene Expression Omnibus (GEO) and BioConductor. *Bioinformatics*. 2007;23(14):1846-7.
29. Bhattacharya S, Dunn P, Thomas CG, Smith B, Schaefer H, Chen J, et al. ImmPort, toward repurposing of open access immunological assay data for translational and clinical research. *Sci Data*. 2018;5:180015.
30. Ritchie ME, Phipson B, Wu D, Hu Y, Law CW, Shi W, et al. Limma powers differential expression analyses for RNA-sequencing and microarray studies. *Nucleic Acids Res*. 2015;43(7):e47.
31. Ashburner M, Ball CA, Blake JA, Botstein D, Butler H, Cherry JM, et al. Gene ontology: Tool for the unification of biology. The Gene Ontology Consortium. *Nat Genet*. 2000;25(1):25-9.
32. Kanehisa M, Goto S. KEGG: kyoto encyclopedia of genes and genomes. *Nucleic Acids Res*. 2000;28(1):27-30.
33. Yu G, Wang LG, Yan GR, He QY. DOSE: An R/Bioconductor package for disease ontology semantic and enrichment analysis. *Bioinformatics*. 2015;31(4):608-9.
34. Subramanian A, Tamayo P, Mootha VK, Mukherjee S, Ebert BL, Gillette MA, et al. Gene set enrichment analysis: a knowledge-based approach for interpreting genome-wide expression profiles. *P Natl Acad Sci Usa*. 2005;102(43):15545-50.
35. Yu G, Wang LG, Han Y, He QY. clusterProfiler: An R package for comparing biological themes among gene clusters. *Omics*. 2012;16(5):284-7.

Immune Infiltration Genes Linked to Osteoporosis Prognosis

36. Liberzon A, Birger C, Thorvaldsdottir H, Ghandi M, Mesirov JP, Tamayo P. The Molecular Signatures Database (MSigDB) hallmark gene set collection. *Cell Syst.* 2015;1(6):417-25.
37. Hanzelmann S, Castelo R, Guinney J. GSEA: gene set variation analysis for microarray and RNA-seq data. *Bmc Bioinformatics.* 2013;14:7.
38. Newman AM, Steen CB, Liu CL, Gentles AJ, Chaudhuri AA, Scherer F, et al. Determining cell type abundance and expression from bulk tissues with digital cytometry. *Nat Biotechnol.* 2019;37(7):773-82.
39. Baldwin AJ. Series introduction: the transcription factor NF-kappaB and human disease. *J Clin Invest.* 2001;107(1):3-6.
40. Soifer HS, Rossi JJ, Saetrom P. MicroRNAs in disease and potential therapeutic applications. *Mol Ther.* 2007;15(12):2070-9.
41. Chang L, Zhou G, Soufan O, Xia J. miRNet 2.0: network-based visual analytics for miRNA functional analysis and systems biology. *Nucleic Acids Res.* 2020;48(W1)W244-51.
42. Shannon P, Markiel A, Ozier O, Baliga NS, Wang JT, Ramage D, et al. Cytoscape: a software environment for integrated models of biomolecular interaction networks. *Genome Res.* 2003;13(11):2498-504.
43. Robin X, Turck N, Hainard A, Tiberti N, Lisacek F, Sanchez JC, et al. pROC: an open-source package for R and S+ to analyze and compare ROC curves. *Bmc Bioinformatics.* 2011;12:77.
44. Che J, Yang J, Zhao B, Shang P. HO-1: A new potential therapeutic target to combat osteoporosis. *Eur J Pharmacol.* 2021;906:174219.
45. Liu X, Ji C, Xu L, Yu T, Dong C, Luo J. Hmox1 promotes osteogenic differentiation at the expense of reduced adipogenic differentiation induced by BMP9 in C3H10T1/2 cells. *J Cell Biochem.* 2018;119(7):5503-16.
46. Bak SU, Kim S, Hwang HJ, Yun JA, Kim WS, Won MH, et al. Heme oxygenase-1 (HO-1)/carbon monoxide (CO) axis suppresses RANKL-induced osteoclastic differentiation by inhibiting redox-sensitive NF-kappaB activation. *Bmb Rep.* 2017;50(2):103-8.
47. Xiao L, Zhong M, Huang Y, Zhu J, Tang W, Li D, et al. Puerarin alleviates osteoporosis in the ovariectomy-induced mice by suppressing osteoclastogenesis via inhibition of TRAF6/ROS-dependent MAPK/NF-kappaB signaling pathways. *Aging (Albany NY).* 2020;12(21):21706-29.
48. Charoanpanich A, Wall ME, Tucker CJ, Andrews DM, Lalush DS, Dirschl DR, et al. Cyclic tensile strain enhances osteogenesis and angiogenesis in mesenchymal stem cells from osteoporotic donors. *Tissue Eng Pt A.* 2014;20(1-2):67-78.
49. Yu T, You X, Zhou H, He W, Li Z, Li B, et al. MiR-16-5p regulates postmenopausal osteoporosis by directly targeting VEGFA. *Aging (Albany NY).* 2020;12(10):9500-14.
50. Armas LA, Recker RR. Pathophysiology of osteoporosis: new mechanistic insights. *Endocrin Metab Clin.* 2012;41(3):475-86.
51. Weitzmann MN. Bone and the Immune System. *Toxicol Pathol.* 2017;45(7):911-24.
52. Saxena Y, Routh S, Mukhopadhyaya A. Immunoporosis: Role of Innate Immune Cells in Osteoporosis. *Front Immunol.* 2021;12:687037.
53. Ng PY, Brigitte PRA, Pavlos NJ. Membrane trafficking in osteoclasts and implications for osteoporosis. *Biochem Soc T.* 2019;47(2):639-50.
54. Lee BS. Myosins in Osteoclast Formation and Function. *Biomolecules.* 2018;8(4)
55. Han G, Zuo J, Holliday LS. Specialized Roles for Actin in Osteoclasts: Unanswered Questions and Therapeutic Opportunities. *Biomolecules.* 2019;9(1):17.
56. Ochiai S, Nishida Y, Higuchi Y, Morita D, Makida K, Seki T, et al. Short-range UV-LED irradiation in postmenopausal osteoporosis using ovariectomized mice. *Sci Rep-Uk.* 2021;11(1):7875.
57. Morita D, Higuchi Y, Makida K, Seki T, Ikuta K, Ishiguro N, et al. Effects of ultraviolet irradiation with a LED device on bone metabolism associated with vitamin D deficiency in senescence-accelerated mouse P6. *Heliyon.* 2020;6(2):e03499.
58. Garcia-Alles LF, Giacometti G, Versluis C, Maveyraud L, de Paepe D, Guiard J, et al. Crystal structure of human CD1e reveals a groove suited for lipid-exchange processes. *P Natl Acad Sci Usa.* 2011;108(32):13230-5.
59. During A. Osteoporosis: A role for lipids. *Biochimie.* 2020;178:49-55.
60. Zhao H, Li Y, Zhang M, Qi L, Tang Y. Blood lipid levels in patients with osteopenia and osteoporosis: A systematic review and meta-analysis. *J Bone Miner Metab.* 2021;39(3):510-20.
61. Mocsai A, Ruland J, Tybulewicz VL. The SYK tyrosine kinase: A crucial player in diverse biological functions. *Nat Rev Immunol.* 2010;10(6):387-402.
62. Csete D, Simon E, Alatschan A, Aradi P, Dobo-Nagy C, Jakus Z, et al. Hematopoietic or Osteoclast-Specific Deletion of Syk Leads to Increased Bone Mass in Experimental Mice. *Front Immunol.* 2019;10:937.

63. Jia Y, Tao Y, Lv C, Xia Y, Wei Z, Dai Y. Tetrandrine enhances the ubiquitination and degradation of Syk through an AhR-c-src-c-Cbl pathway and consequently inhibits osteoclastogenesis and bone destruction in arthritis. *Cell Death Dis.* 2019;10(2):38.
64. Xie G, Liu W, Lian Z, Xie D, Yuan G, Ye J, et al. Spleen tyrosine kinase (SYK) inhibitor PRT062607 protects against ovariectomy-induced bone loss and breast cancer-induced bone destruction. *Biochem Pharmacol.* 2021;188:114579.